Eidgenössische Technische Hochschule Zürich

Ecole polytechnique fédérale de Zurich
Politecnico federale di Zurigo
Swiss Federal Institute of Technology Zurich

Mixed hp-DGFEM for incompressible flows III: Pressure stabilization*

D. Schötzau†, Ch. Schwab and A. Toselli

Research Report No. 2002-25
December 2002

Seminar für Angewandte Mathematik
Eidgenössische Technische Hochschule
CH-8092 Zürich
Switzerland

*The first author was partially supported by the Swiss National Science Foundation under Project 21-068126.02. The last two authors were partially supported by the Swiss National Science Foundation under Project 20-63397.00

†Department of Mathematics, University of Basel, Rheinsprung 21, CH-4051 Basel, Switzerland, email: schotzau@math.unibas.ch

Mixed hp-DGFEM for incompressible flows III: Pressure stabilization*

D. Schötzau†, Ch. Schwab and A. Toselli

Seminar für Angewandte Mathematik
Eidgenössische Technische Hochschule
CH-8092 Zürich
Switzerland

Research Report No. 2002-25 December 2002

Abstract

We consider stabilized mixed *hp*-discontinuous Galerkin methods for the discretization of the Stokes problem in three-dimensional polyhedral domains. The methods are stabilized with a term penalizing the pressure jumps. For this approach it is shown that $\mathbb{Q}_k - \mathbb{Q}_k$ and $\mathbb{Q}_k - \mathbb{Q}_{k-1}$ elements satisfy a generalized inf-sup condition on geometric edge and boundary layer meshes that are refined anisotropically and non quasi-uniformly towards faces, edges, and corners. The discrete inf-sup constant is proven to be independent of the aspect ratios of the anisotropic elements and to decrease as $k^{-1/2}$ with the approximation order. We also show that the generalized inf-sup condition leads to a global stability result in a suitable energy norm.

Keywords: *hp*-FEM, discontinuous Galerkin methods, Stokes problem, anisotropic refinement

AMS Subject Classification: 65N30, 65N35, 65N12, 65N15

*The first author was partially supported by the Swiss National Science Foundation under Project 21-068126.02. The last two authors were partially supported by the Swiss National Science Foundation under Project 20-63397.00

†Department of Mathematics, University of Basel, Rheinsprung 21, CH-4051 Basel, Switzerland, email: schotzau@math.unibas.ch

1 Introduction

Over the last few years, several discontinuous Galerkin (DG) methods for incompressible flow problems and for certain saddle-point problems with incompressibility constraints have been proposed in the literature. Here we only mention the piecewise solenoidal discontinuous Galerkin methods introduced in [6, 20], the local discontinuous Galerkin (LDG) methods of [11, 10], and the interior penalty methods studied in [18, 29, 17]. The methods above all rely on discrete velocity spaces consisting of piecewise polynomial functions with no kind of continuity constraints between the elements in the underlying triangulation. Interelemental communication is achieved through so-called numerical fluxes, as in the original discontinuous Galerkin methods for non-linear hyperbolic systems; see [12, 9, 13] and the references therein. The main motivations for using DG methods in fluid flow problems lie in their robustness in convection-dominated regimes, their conservation properties, and their great flexibility in the mesh-design. Based on completely discontinuous finite element spaces, DG methods easily handle elements of various types and shapes, non-matching grids and even local spaces of different orders; they are therefore ideal for *hp*-adaptivity.

Even if transport phenomena may be dominant in incompressible flow problems, mixed DG methods still require suitable velocity-pressure pairs in order to ensure stability and convergence of the underlying Stokes discretization. In [18, 29], it was shown that discontinuous $\mathbb{P}_k - \mathbb{P}_{k-1}$ and $\mathbb{Q}_k - \mathbb{Q}_{k-1}$ pairs are inf-sup stable with respect to the mesh-size, as opposed to their conforming counterparts. These elements are optimal from an approximation point of view. A slightly different approach was proposed in [11, 10]. There, the introduction of a pressure stabilization term was proven to also render the convenient equal-order $\mathbb{P}_k - \mathbb{P}_k$ and $\mathbb{Q}_k - \mathbb{Q}_k$ elements stable, uniformly in the mesh-size.

The study of mixed *hp*-discontinuous Galerkin methods was initiated in [29] where several discontinuous velocity-pressure pairs were shown to possess better stability properties than their conforming versions. In particular, the numerical results reported there for two-dimensional uniform meshes show that discontinuous $\mathbb{Q}_k - \mathbb{Q}_{k-1}$ elements are also uniformly stable with respect to the polynomial degree k. For this pair, the best available bound of the inf-sup constant in terms of k was then obtained in [24] and decreases as k^{-1}, on shape-regular tensor-product meshes in two and three dimensions, possibly with hanging nodes. This bound ensures the same p-version convergence rate for the velocity and the pressure as that of conforming $\mathbb{Q}_k - \mathbb{Q}_{k-2}$ elements in three dimensions. However, the latter elements are mismatched with respect to h-approximation.

In laminar regimes, solutions of incompressible flow problems in polyhedral domains have corner and edge singularities. In addition, strong boundary layers may arise at faces, edges, and corners. In the *hp*-version of the finite element method, these solution components can be approximated at exponential rate of convergence provided that the meshes are geometrically and anisotropically graded towards faces, edges, and corners; see [2, 5, 21, 27, 28] and the references therein. These anisotropically refined meshes raise serious stability issues in mixed approximations as the inf-sup constants might in general be very sensi-

tive to the aspect ratios of the elements. It has recently been shown for two- and three-dimensional conforming approximations employing $\mathbb{Q}_k - \mathbb{Q}_{k-2}$ elements that, on corner, edge, and boundary-layer tensor-product meshes, the inf-sup constant for the Stokes problem is in fact independent of the aspect ratios of the anisotropic elements in the meshes; see [22, 23, 1, 30] and the references therein. In the more recent work [25], discontinuous $\mathbb{Q}_k - \mathbb{Q}_{k-1}$ elements have been studied on geometric edge meshes designed to resolve corner and edge singularities in the absence of boundary layers. By suitably defining the discontinuity stabilization parameters in the DG bilinear forms on anisotropic elements, it has been proven that this velocity-pressure pair is divergence stable, with an inf-sup constant that is independent of the aspect ratios of the anisotropic elements and that decrease as $k^{-3/2}$ in the approximation order.

In this paper, we continue our study of the stability properties of mixed *hp*-DGFEM for the Stokes problem started in [29, 24, 25], and analyze stabilized variants thereof on geometric meshes in three dimensions. We show that the introduction of the pressure stabilization term originally proposed in the LDG discretization in [11] leads to a generalized inf-sup constant for $\mathbb{Q}_k - \mathbb{Q}_{k-1}$ and $\mathbb{Q}_k - \mathbb{Q}_k$ elements that decreases only as $k^{-1/2}$ in the polynomial degree, and is independent of possibly large aspect ratios of the mesh. As opposed to the work in [25] that only considers geometric edge meshes, the results here also hold for geometric boundary layer meshes that are additionally geometrically refined towards the faces. As a consequence of the generalized inf-sup condition, we obtain a global stability result in a suitable energy norm and derive *p*-version error bounds that are better than those in [24], by of half an order of k in the velocity and a full order of k in the pressure, respectively. We emphasize that, in our analysis, we use a similar unifying setting as that proposed in [24]. Thus, although we only consider the so-called interior penalty discontinuous Galerkin method, our results hold true verbatim for the analogs of the methods analyzed in [24], and, in particular, extend the *h*-analysis in [11] to the *hp*-context.

The outline of the paper is as follows. In section 2, we introduce stabilized mixed *hp*-DGFEM methods for the Stokes problem. Two classes of geometric meshes are defined in section 3. Continuity and coercivity properties of the DG forms on these meshes are established in section 4. Our main result is the generalized inf-sup condition that we present and prove in section 5. A global stability result for the proposed DG discretizations is then derived in section 6, together with *hp*-error bounds on shape-regular elements.

2 Stabilized mixed hp-DGFEM for the Stokes problem

In this section, we introduce stabilized mixed *hp*-discontinuous Galerkin methods using the pressure stabilization form that was originally proposed for the LDG discretization in [11].

2.1 The Stokes problem

Let Ω be a bounded polyhedron in $\mathbb{R}^3$, and let $\mathbf{n}$ be the outward normal unit vector to its boundary $\partial\Omega$. Given a source term $\mathbf{f} \in L^2(\Omega)^3$ and a Dirichlet datum $\mathbf{g} \in H^{1/2}(\partial\Omega)^3$ with $\int_{\partial\Omega} \mathbf{g} \cdot \mathbf{n}\, ds = 0$, the Stokes problem consists in finding a velocity field $\mathbf{u}$ and a pressure p such that

$$\begin{aligned} -\nu\Delta\mathbf{u} + \nabla p &= \mathbf{f} && \text{in } \Omega, \\ \nabla \cdot \mathbf{u} &= 0 && \text{in } \Omega, \\ \mathbf{u} &= \mathbf{g} && \text{on } \partial\Omega. \end{aligned} \tag{1}$$

Thanks to the inf-sup condition

$$\inf_{0 \neq q \in L^2(\Omega)/\mathbb{R}} \sup_{\mathbf{0} \neq \mathbf{v} \in H_0^1(\Omega)^3} \frac{-\int_\Omega q\, \nabla \cdot \mathbf{v}\, d\mathbf{x}}{|\mathbf{v}|_1 \|q\|_0} \geq C_\Omega > 0, \tag{2}$$

with a constant C_Ω depending only on Ω (see, e.g., [7, 16]), the Stokes problem (1) has a unique solution $(\mathbf{u}, p)$ with

$$\mathbf{u} \in \mathbf{V} := H^1(\Omega)^3, \qquad p \in Q := L_0^2(\Omega) = L^2(\Omega)/\mathbb{R}.$$

Here, we denote by $\|\cdot\|_{s,\mathcal{D}}$ and $|\cdot|_{s,\mathcal{D}}$ the norm and seminorm of the Sobolev space $H^s(\mathcal{D})$, $s \geq 0$ on a domain $\mathcal{D}$ in $\mathbb{R}^d$, $d = 1, 2, 3$. The same notation is used to denote norms for vector fields. In case $\mathcal{D} = \Omega$, we drop the subscript.

2.2 Meshes and trace operators

Throughout, we consider triangulations $\mathcal{T}$ on Ω that consist of affine hexahedral elements $\{K\}$. More precisely, each element $K \in \mathcal{T}$ is obtained from the reference cube $\widehat{Q} = (-1, 1)^3$ by an affine mapping. In general, we allow for *irregular* meshes, i.e., meshes with hanging nodes (see [26, Sect. 4.4.1]), but suppose that the intersection between neighboring elements is either a common vertex, a common edge, a common face, or an entire face of one of the two elements. An interior face of $\mathcal{T}$ is the (non-empty) two-dimensional interior of $\partial K^+ \cap \partial K^-$, where K^+ and K^- are two adjacent elements of $\mathcal{T}$. Similarly, a boundary face of $\mathcal{T}$ is the (non-empty) two-dimensional interior of $\partial K \cap \partial\Omega$ which consists of entire faces of ∂K. We denote by $\mathcal{F}_\mathcal{I}$ the union of all interior faces of $\mathcal{T}$, by $\mathcal{F}_\mathcal{B}$ the union of all boundary faces, and set $\mathcal{F} = \mathcal{F}_\mathcal{I} \cup \mathcal{F}_\mathcal{B}$.

For an element $K \in \mathcal{T}$, we denote its diameter by h_K and the radius of the biggest circle that can be inscribed into K by ρ_K. A mesh $\mathcal{T}$ is called *shape-regular* if

$$h_K \leq c\rho_K, \qquad \forall K \in \mathcal{T}, \tag{3}$$

for a shape-regularity constant $c > 0$ that is independent of the elements. Our meshes are not necessarily shape-regular; see section 3.

We next define some trace operators. Let $f \subset \mathcal{F}_\mathcal{I}$ be an interior face shared by two elements K^+ and K^- and $\mathbf{v}$, q, and $\underline{\tau}$ be vector-, scalar- and matrix-valued functions, respectively, that are smooth inside each element $K^\pm$. We

denote by $\mathbf{v}^{\pm}$, $q^{\pm}$ and $\underline{\tau}^{\pm}$ the traces of $\mathbf{v}$, q and $\underline{\tau}$ on f from the interior of $K^{\pm}$ and define the mean values $\{\!\{\cdot\}\!\}$ and normal jumps $[\![\cdot]\!]$ at $\mathbf{x} \in f$ as

$$\begin{aligned} \{\!\{\mathbf{v}\}\!\} &:= (\mathbf{v}^+ + \mathbf{v}^-)/2, & [\![\mathbf{v}]\!] &:= \mathbf{v}^+ \cdot \mathbf{n}_{K^+} + \mathbf{v}^- \cdot \mathbf{n}_{K^-}, \\ \{\!\{q\}\!\} &:= (q^+ + q^-)/2, & [\![q]\!] &:= q^+ \, \mathbf{n}_{K^+} + q^- \, \mathbf{n}_{K^-}, \\ \{\!\{\underline{\tau}\}\!\} &:= (\underline{\tau}^+ + \underline{\tau}^-)/2, & [\![\underline{\tau}]\!] &:= \underline{\tau}^+ \mathbf{n}_{K^+} + \underline{\tau}^- \mathbf{n}_{K^-}. \end{aligned}$$

Here, we denote by $\mathbf{n}_K$ the outward normal unit vector to the boundary ∂K of an element K. We also define the matrix-valued jump of the velocity $\mathbf{v}$ given by

$$\underline{[\![\mathbf{v}]\!]} := \mathbf{v}^+ \otimes \mathbf{n}_{K^+} + \mathbf{v}^- \otimes \mathbf{n}_{K^-},$$

where, for two vectors $\mathbf{a}$ and $\mathbf{b}$, $[\mathbf{a} \otimes \mathbf{b}]_{ij} = a_i b_j$. On a boundary face $f \subset \mathcal{F}_{\mathcal{B}}$ given by $f = \partial K \cap \partial\Omega$, we set $\{\!\{\mathbf{v}\}\!\} := \mathbf{v}$, $\{\!\{q\}\!\} := q$, $\{\!\{\underline{\tau}\}\!\} := \underline{\tau}$, as well as $[\![\mathbf{v}]\!] := \mathbf{v} \cdot \mathbf{n}$, $\underline{[\![\mathbf{v}]\!]} := \mathbf{v} \otimes \mathbf{n}$, $[\![q]\!] := q\mathbf{n}$ and $[\![\tau]\!] := \tau \cdot \mathbf{n}$.

2.3 Finite element spaces

Given a mesh $\mathcal{T}$ on Ω and an approximation order $k \geq 0$, we introduce the finite element spaces $\mathbf{V}_h^k(\mathcal{T})$ and $Q_h^k(\mathcal{T})$:

$$\begin{aligned} \mathbf{V}_h^k(\mathcal{T}) &:= \{\, \mathbf{v} \in L^2(\Omega)^3 : \mathbf{v}|_K \in \mathbb{Q}_k(K)^3, \ K \in \mathcal{T} \,\}, \\ Q_h^k(\mathcal{T}) &:= \{\, q \in L_0^2(\Omega) : q|_K \in \mathbb{Q}_k(K), \ K \in \mathcal{T} \,\}, \end{aligned} \tag{4}$$

where $\mathbb{Q}_k(K)$ is the space of polynomials of maximum degree k in each variable on K.

2.4 Mixed discontinuous Galerkin approximations

We approximate the velocities and pressures in the spaces $\mathbf{V}_h$ and Q_h given by

$$\mathbf{V}_h := \mathbf{V}_h^k(\mathcal{T}), \qquad Q_h := Q_h^\ell(\mathcal{T}), \tag{5}$$

with $k \geq 1$ and $\ell = k$ or $\ell = k - 1$. We refer to these velocity-pressure pairs as (non-conforming) equal-order $\mathbb{Q}_k - \mathbb{Q}_k$ elements and mixed-order $\mathbb{Q}_k - \mathbb{Q}_{k-1}$ elements, respectively.

We consider the following stabilized mixed DG methods: find $(\mathbf{u}_h, p_h) \in \mathbf{V}_h \times Q_h$ such that

$$\left\{ \begin{array}{rcrcl} A_h(\mathbf{u}_h, \mathbf{v}) & + & B_h(\mathbf{v}, p_h) & = & F_h(\mathbf{v}) \\ -B_h(\mathbf{u}_h, q) & + & C_h(p_h, q) & = & G_h(q) \end{array} \right. \tag{6}$$

for all $(\mathbf{v}, q) \in \mathbf{V}_h \times Q_h$. The forms A_h, B_h, and C_h are

$$\begin{aligned} A_h(\mathbf{u},\mathbf{v}) &= \int_\Omega \nu\nabla_h\mathbf{u} : \nabla_h\mathbf{v}\, d\mathbf{x} - \int_{\mathcal{F}} \left(\{\!\{\nu\nabla_h\mathbf{v}\}\!\} : \underline{[\![\mathbf{u}]\!]} + \{\!\{\nu\nabla_h\mathbf{u}\}\!\} : \underline{[\![\mathbf{v}]\!]} \right) ds \\ &\quad + \nu \int_{\mathcal{F}} \delta\, \underline{[\![\mathbf{u}]\!]} : \underline{[\![\mathbf{v}]\!]}\, ds, \\ B_h(\mathbf{v},q) &= -\int_\Omega q\, \nabla_h \cdot \mathbf{v}\, d\mathbf{x} + \int_{\mathcal{E}} \{\!\{q\}\!\}[\![\mathbf{v}]\!]\, ds, \\ C_h(p,q) &= \nu^{-1} \int_{\mathcal{F}_{\mathcal{I}}} \gamma\, [\![p]\!][\![q]\!]\, ds. \end{aligned}$$

Here, ∇_h is the discrete gradient, taken elementwise. The functions $\delta \in L^\infty(\mathcal{F})$ and $\gamma \in L^\infty(\mathcal{F}_{\mathcal{I}})$ are the so-called discontinuity and pressure stabilization functions, respectively, for which we will make a precise choice in section 3.3. Finally, the corresponding right-hand sides F_h and G_h are

$$\begin{aligned} F_h(\mathbf{v}) &= \int_\Omega \mathbf{f}\cdot\mathbf{v}\, d\mathbf{x} - \int_{\mathcal{F}_{\mathcal{B}}} (\mathbf{g}\otimes\mathbf{n}) : \{\!\{\nu\nabla_h\mathbf{v}\}\!\}\, ds + \nu \int_{\mathcal{F}_{\mathcal{B}}} \delta\, \mathbf{g}\cdot\mathbf{v}\, ds, \\ G_h(q) &= -\int_{\mathcal{F}_{\mathcal{B}}} q\, \mathbf{g}\cdot\mathbf{n}\, ds. \end{aligned}$$

Remark 2.1. *It follows from the stability results in section 6 below that problem (6) has a unique solution* $(\mathbf{u}_h, p_h) \in \mathbf{V}_h \times Q_h$.

Remark 2.2. *The form* $A_h(\cdot,\cdot)$ *discretizing the Laplacian is the so-called interior penalty (IP) form. Several other choices are possible for* $A_h(\cdot,\cdot)$*, as discussed in [24]. All the results of this paper also hold verbatim for the forms considered there. The form* $B_h(\cdot,\cdot)$ *is related to the incompressibility constraint; it is used in the mixed DG approaches in [11, 18, 29, 24, 17]. Finally,* $C_h(\cdot,\cdot)$ *is the pressure stabilization form that was originally introduced in the local discontinuous Galerkin methods in [11, 10].*

2.5 Perturbed mixed formulation

For the purpose of the analysis, we introduce perturbed forms $\widetilde{A}_h$ and $\widetilde{B}_h$, following the ideas in [4, 24]. To this end, we define the space $\mathbf{V}(h) := \mathbf{V} + \mathbf{V}_h$, and introduce the lifting operators $\mathcal{L} : \mathbf{V}(h) \to \underline{\Sigma}_h$ and $\mathcal{M} : \mathbf{V}(h) \to Q_h$ by

$$\begin{aligned} \int_\Omega \underline{\mathcal{L}}(\mathbf{v}) : \underline{\tau}\, d\mathbf{x} &= \int_{\mathcal{F}} \underline{[\![\mathbf{v}]\!]} : \{\!\{\underline{\tau}\}\!\}\, ds, \qquad \forall \underline{\tau} \in \underline{\Sigma}_h, \\ \int_\Omega \mathcal{M}(\mathbf{v}) q\, d\mathbf{x} &= \int_{\mathcal{E}} [\![\mathbf{v}]\!]\{\!\{q\}\!\}\, ds, \qquad \forall q \in Q_h, \end{aligned}$$

where we use the auxiliary space $\underline{\Sigma}_h = \{\, \underline{\tau} \in L^2(\Omega)^{3\times 3} : \underline{\tau}|_K \in \mathbb{Q}_k(K)^{3\times 3},\ K \in \mathcal{T}\,\}$. We then introduce the following perturbed forms on $\mathbf{V}(h) \times \mathbf{V}(h)$ and

$\mathbf{V}(h) \times Q$:

$$\widetilde{A}_h(\mathbf{u},\mathbf{v}) = \int_\Omega \nu\big[\nabla_h\mathbf{u} : \nabla_h\mathbf{v} - \underline{\mathcal{L}}(\mathbf{u}) : \nabla_h\mathbf{v} - \underline{\mathcal{L}}(\mathbf{v}) : \nabla_h\mathbf{u}\big]\, d\mathbf{x} + \nu \int_{\mathcal{F}} \delta \underline{[\![\mathbf{u}]\!]} : \underline{[\![\mathbf{v}]\!]}\, ds,$$
$$\widetilde{B}_h(\mathbf{v},q) = -\int_\Omega q\,[\nabla_h \cdot \mathbf{v} - \mathcal{M}(\mathbf{v})]\, d\mathbf{x}. \tag{7}$$

We have

$$\widetilde{A}_h = A_h \text{ on } \mathbf{V}_h \times \mathbf{V}_h, \qquad \widetilde{B}_h = B_h \text{ on } \mathbf{V}_h \times Q_h.$$

Thus, we may rewrite the method (6) as: find $(\mathbf{u}_h, p_h) \in \mathbf{V}_h \times Q_h$ such that

$$\left\{ \begin{array}{rcrcl} \widetilde{A}_h(\mathbf{u}_h,\mathbf{v}) & + & \widetilde{B}_h(\mathbf{v},p_h) & = & F_h(\mathbf{v}) \\ -\widetilde{B}_h(\mathbf{u}_h,q) & + & C_h(p_h,q) & = & G_h(q) \end{array} \right. \tag{8}$$

for all $(\mathbf{v},q) \in \mathbf{V}_h \times Q_h$.

3 Geometric edge and boundary layer meshes

In this section, we define two classes of *geometric meshes*, namely *geometric edges meshes* that are employed in the presence of corner and edge singularities (as, e.g., in Stokes flow or nearly incompressible elasticity), and *geometric boundary layer meshes* that are used when, in addition to corner/edge singularities, boundary layers are present as well. Both meshes are characterized by a *geometric grading factor* $\sigma \in (0,1)$ and the *number of layers* n, the thinnest layer having width proportional to σ^n. We refer to [2, 5, 21, 27, 28, 30] and the references therein for a more detailed discussion on how to choose these parameters in order to resolve singularities and layers at exponential rates of convergence.

3.1 Geometric edge meshes

A *geometric edge mesh* $\mathcal{T}_{edge}^{n,\sigma}$ is constructed by considering an initial shape-regular macro-triangulation $\mathcal{T}_m = \{M\}$ of Ω, with no hanging nodes, possibly consisting of just one element. The macro-elements M in the interior of Ω are then refined isotropically and regularly (not discussed further) while the macro-elements M on the boundary of Ω are refined geometrically and anisotropically towards edges and corners. This geometric refinement is obtained by affinely mapping corresponding reference triangulations (referred to as *patches*) on $\widehat{Q}$ onto the macro-elements M using the elemental maps $F_M : \widehat{Q} \to M$. This process is illustrated in Figure 1. For edge meshes, the following patches on $\widehat{Q} = I^3$, $I = (-1,1)$, are used for the geometric refinement towards the boundary of Ω:

Edge patches: An edge patch $\mathcal{T}_e^{edge}$ on $\widehat{Q}$ is given by

$$\mathcal{T}_e^{edge} := \{K_{xy} \times I \mid \quad K_{xy} \in \mathcal{T}_{xy}\},$$

where $\mathcal{T}_{xy}$ is an irregular corner mesh, geometrically refined towards a vertex of $\widehat{S} = (-1,1)^2$ with grading factor σ and n refinement levels; see Figure 1 (level 2, left).

Corner patches: In order to build a corner patch $\mathcal{T}_c^{edge}$ on $\widehat{Q}$, we first consider an initial, irregular, corner mesh $\mathcal{T}_{c,m}$, geometrically refined towards a vertex of $\widehat{Q}$, with grading factor σ and n refinement levels; see the mesh in bold lines in Figure 1 (level 2, right). The elements of this mesh are then irregularly refined towards the three edges adjacent to the vertex in order to obtain the mesh $\mathcal{T}_c^{edge}$; see also Figure 3.

For simplicity, we always assume that the only hanging nodes in geometric edge meshes $\mathcal{T}_{edge}^{n,\sigma}$ are those in the closure of edge and corner patches.

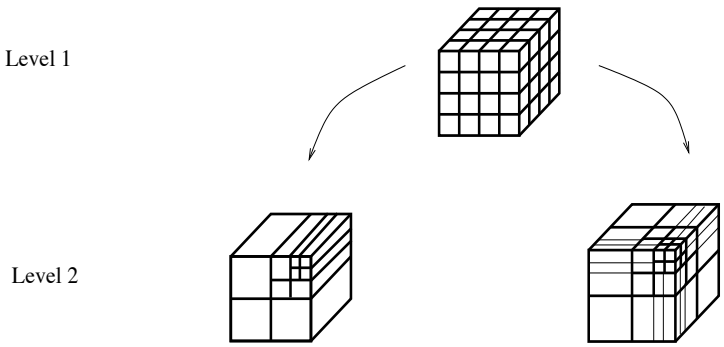

Figure 1: Hierarchic structure of a geometric edge mesh $\mathcal{T}_{edge}^{n,\sigma}$. The macro-elements M on the boundary of Ω (level 1) are further refined as edge and corner patches (level 2). The geometric grading factor is here $\sigma = 0.5$.

3.2 Geometric boundary layer meshes

As for edge meshes, the construction of a *geometric boundary layer mesh* $\mathcal{T}_{bl}^{n,\sigma}$ starts from an initial shape-regular macro-triangulation $\mathcal{T}_m = \{M\}$ of Ω, with no hanging nodes, possibly consisting of just one element. The macro-elements M on the boundary of Ω are now also refined geometrically towards faces; see in Figure 2. More precisely, the following face, edge, and corner patches on $\widehat{Q} = I^3$ are used:

Face patches: A face patch $\mathcal{T}_f^{bl}$ on $\widehat{Q}$ is given by an anisotropic triangulation of the form

$$\mathcal{T}_f^{bl} := \{K_x \times I \times I \mid \quad K_x \in \mathcal{T}_x\},$$

where $\mathcal{T}_x$ is a mesh of I, geometrically refined towards one of the vertices, say $x = 1$, with grading factor $\sigma \in (0,1)$ and total number of layers n; see Figure 2 (level 2, left).

Edge patches: An edge patch $\mathcal{T}_e^{bl}$ on $\widehat{Q}$ is given by

$$\mathcal{T}_e^{bl} := \{K_{xy} \times I \mid \quad K_{xy} \in \widetilde{\mathcal{T}}_{xy}\},$$

where $\widetilde{\mathcal{T}}_{xy}$ is a triangulation of $\widehat{S} = I^2$ obtained by first considering an irregular corner mesh $\mathcal{T}_{xy}$ as in a patch $\mathcal{T}_e^{edge}$ of an edge mesh, geometrically refined towards a vertex of $\widehat{S}$, say $(x, y) = (1, 1)$, with grading factor σ and n refinement levels (see Figure 1 below, level 2, left). The elements of the mesh $\mathcal{T}_{xy}$ are then anisotropically refined towards the two edges $x = 1$ and $y = 1$, in order to obtain a regular mesh $\widetilde{\mathcal{T}}_{xy}$. We refer to Figure 2 (level 2, center) for an example.

Corner patches: In order to build a corner patch $\mathcal{T}_c^{bl}$ on $\widehat{Q}$, we first consider the same initial, irregular corner mesh $\mathcal{T}_{c,m}$, geometrically refined towards a vertex of $\widehat{Q}$, with grading factor σ and n refinement levels; see the mesh in bold lines in Figure 2 (level 2, right). The elements of $\mathcal{T}_{c,m}$ are then anisotropically refined towards the three faces $x = 1$, $y = 1$, and $z = 1$ in order to obtain a regular mesh $\mathcal{T}_c^{bl}$; see also Figure 3.

For simplicity, we always assume that the three types of patches above are combined in such a way that geometric boundary layer meshes $\mathcal{T}_{bl}^{n,\sigma}$ do not contain hanging nodes.

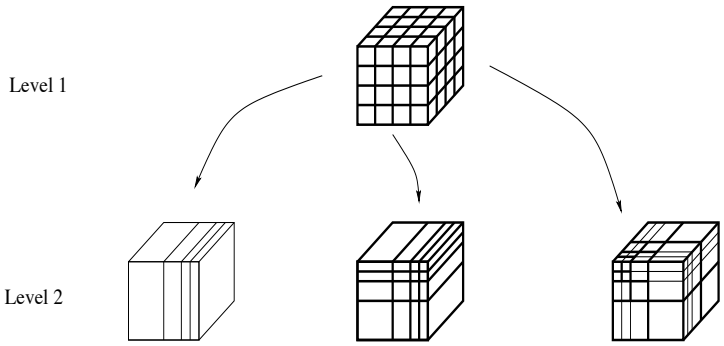

Figure 2: Hierarchic structure of a geometric boundary layer mesh $\mathcal{T}_{bl}^{n,\sigma}$. The macro-elements M on the boundary of Ω (level 1) are further refined as face, edge and corner patches (level 2). The geometric grading factor is here $\sigma = 0.5$.

Remark 3.1. *We note that the underlying mesh $\mathcal{T}_{c,m}$ is the same for the corner patches $\mathcal{T}_c^{edge}$ and $\mathcal{T}_c^{bl}$ in edge and boundary layer meshes, respectively. However, $\mathcal{T}_c^{edge}$ is irregular and contains hanging nodes. Figure 3 shows the difference between corner patches for boundary layer and edge meshes.*

The geometric edge and boundary layer meshes defined above satisfy the following property; see [25, Sect. 3].

Figure 3: Geometrically refined corner patches $\mathcal{T}_c^{bl}$ and $\mathcal{T}_c^{edge}$ for boundary layer (left) and edge (right) meshes. The geometric grading factor is $\sigma = 0.5$.

Property 3.1. *Let $\mathcal{T}$ be a geometric edge mesh $\mathcal{T}_{edge}^{n,\sigma}$ or a geometric boundary layer mesh $\mathcal{T}_{bl}^{n,\sigma}$, with a grading factor $\sigma \in (0,1)$ and n levels of refinement. Then, any $K \in \mathcal{T}$ can be written as $K = F_K(K_{xyz})$, where K_{xyz} is of the form*

$$K_{xyz} = I_x \times I_y \times I_z = (x_1, x_2) \times (y_1, y_2) \times (z_1, z_2),$$

and F_K is an affine mapping, the Jacobian of which satisfies

$$|\det(J_K)| \leq C, \qquad |\det(J_K^{-1})| \leq C, \qquad \|DF_K\| \leq C, \qquad \|DF_K^{-1}\| \leq C,$$

with constants only depending on the angles of K but not on its dimensions.

We note that the constants in Property 3.1 only depend on the shape-regularity constant in (3) of the underlying macro-element mesh $\mathcal{T}_m$. The dimensions of K_{xyz} on the other hand may depend on the geometric grading factor and the number of refinements.

For an element K of a geometric edge mesh, we define, according to Property 3.1,

$$h_x^K = h_x = x_2 - x_1, \quad h_y^K = h_x = y_2 - y_1, \quad h_z^K = h_x = z_2 - z_1.$$

3.3 Stabilization on geometric meshes

In this section, we define the discontinuity and pressure stabilization functions $\delta \in L^\infty(\mathcal{F})$ and $\gamma \in L^\infty(\mathcal{F}_\mathcal{I})$ on geometric meshes.

To this end, let f be an entire face of an element K of a geometric mesh $\mathcal{T}$ on Ω. According to Property 3.1, K can be obtained by a stretched parallelepiped K_{xyz} by an affine mapping F_K that only changes the angles. Suppose that the face f is the image of, e.g., the face $\{x = x_1\}$. We set $h_f = h_x$. For a face perpendicular to the y- or z-direction, we choose $h_f = h_y$ or $h_f = h_z$, respectively.

Let then K and K' be two elements with entire faces f and f' that share an interior face $f = f \cap f'$ in $\mathcal{F}_{\mathcal{I}}$. We have

$$ch_f \leq h_{f'} \leq c^{-1} h_f, \tag{9}$$

with a constant $c > 0$ that only depends on the geometric grading factor σ and the constant in (3) for the underlying macro-mesh $\mathcal{T}_m$. We define the function $\mathtt{h} \in L^\infty(\mathcal{F})$ by

$$\mathtt{h}(\mathbf{x}) := \begin{cases} \min\{h_f, h_{f'}\} & \mathbf{x} \in f \cap f' \subset \mathcal{F}_{\mathcal{I}}, \\ h_f & \mathbf{x} \in f \subset \mathcal{F}_{\mathcal{B}}. \end{cases} \tag{10}$$

We then set

$$\delta(\mathbf{x}) = \delta_0 \mathtt{h}^{-1} k^2, \qquad \mathbf{x} \in \mathcal{F}, \tag{11}$$

and

$$\gamma(\mathbf{x}) = \gamma_0 \, \min\{h_f, h_{f'}\} \, \max\{1, \ell\}^{-1}, \qquad \mathbf{x} \in \mathcal{F}_{\mathcal{I}}, \tag{12}$$

with $\delta_0 > 0$ and $\gamma_0 > 0$ independent of $\mathtt{h}$ and k.

Remark 3.2. *For isotropically refined, shape-regular meshes, the definitions in (10) and (11) are equivalent to the usual definition of δ, see [24]. Similarly, the definition of γ in (12) generalizes the definition in [11] to the hp-DGFEM context on geometric meshes.*

4 Continuity and coercivity on geometric meshes

On the geometric meshes defined in section 3, the continuity of $\widetilde{A}_h$ and $\widetilde{B}_h$ as well as the coercivity of A_h can be established as in [25, Sect. 4].

To this end, we equip $\mathbf{V}(h) = \mathbf{V} + \mathbf{V}_h$ with the broken norm

$$\|\mathbf{v}\|_h^2 := \sum_{K \in \mathcal{T}} |\mathbf{v}|_{1,K}^2 + \int_{\mathcal{F}} \delta |\underline{[\![\mathbf{v}]\!]}|^2 \, ds, \qquad \mathbf{v} \in \mathbf{V}(h).$$

We have the following result.

Theorem 4.1. *Let $\mathcal{T}$ be a geometric edge mesh $\mathcal{T}_{edge}^{n,\sigma}$ or a geometric boundary layer mesh $\mathcal{T}_{bl}^{n,\sigma}$, with a grading factor $\sigma \in (0,1)$ and n levels of refinement. Let the stabilization functions δ be defined as in (10) and (11). Then, the forms $\widetilde{A}_h$ and $\widetilde{B}_h$ in (7) are continuous:*

$$\begin{aligned} |\widetilde{A}_h(\mathbf{v}, \mathbf{w})| &\leq \nu \alpha_1 \|\mathbf{v}\|_h \|\mathbf{w}\|_h \qquad \forall \, \mathbf{v}, \mathbf{w} \in \mathbf{V}(h), \\ |\widetilde{B}_h(\mathbf{v}, q)| &\leq \alpha_2 \|\mathbf{v}\|_h \|q\|_0 \qquad \forall \, \mathbf{u} \in \mathbf{V}(h), \; q \in Q, \end{aligned}$$

with continuity constants α_1 and α_2 that depend on δ_0 and the constants in Property 3.1, but are independent of ν, k, n, and the aspect ratio of $\mathcal{T}$. Furthermore, there exists a constant $\delta_{\min} > 0$ that depends on the constants in Property

3.1, but is independent of ν, k, n, and the aspect ratio of $\mathcal{T}$, such that, for any $\delta_0 \geq \delta_{\min}$,

$$A_h(\mathbf{v},\mathbf{v}) \geq \nu\beta\|\mathbf{v}\|_h^2 \qquad \forall\, \mathbf{v} \in \mathbf{V}_h,$$

for a coercivity constant $\beta > 0$ depending on δ_0 and the constants in Property 3.1, but independent of ν, k, n, and the aspect ratio of $\mathcal{T}$.

Remark 4.1. *The results in Theorem 4.1 are based on anisotropic stability estimates for the lifting operators $\underline{\mathcal{L}}$ and $\mathcal{M}$ that can be found in [25, Sect. 4]. These operators are identical for all the DG forms considered in [24] and, thus, the results in Theorem 4.1 also hold for all the mixed DG methods considered there. We note that the restriction on δ_0 is typical for the interior penalty form A_h and can be avoided if A_h is chosen to be, e.g., the local discontinuous Galerkin form, the nonsymmetric interior penalty form, or the second Bassi-Rebay form, see [24].*

Next, we address the continuity of F_h and G_h.

Theorem 4.2. *Let $\mathcal{T}$ be a geometric edge mesh $\mathcal{T}_{edge}^{n,\sigma}$ or a geometric boundary layer mesh $\mathcal{T}_{bl}^{n,\sigma}$, with a grading factor $\sigma \in (0,1)$ and n levels of refinement. Let the stabilization functions δ be defined as in (10) and (11). Then we have*

$$|F_h(\mathbf{v})| \leq C\left[\|\mathbf{f}\|_0 + \nu\|\delta^{\frac{1}{2}}\mathbf{g}\|_{0,\partial\Omega}\right]\|\mathbf{v}\|_h \qquad \forall\, \mathbf{v} \in \mathbf{V}_h,$$
$$|G_h(q)| \leq C\,\|\delta^{\frac{1}{2}}\mathbf{g}\|_{0,\partial\Omega}\,\|q\|_0 \qquad \forall\, q \in Q_h,$$

with continuity constants that depend on δ_0, Ω, and the constants in Property 3.1, but are independent of ν, k, n, and the aspect ratio of $\mathcal{T}$.

Proof. We first note that we have the Poincaré inequality

$$\|\mathbf{v}\|_0 \leq C\|\mathbf{v}\|_{1,h} \qquad \forall\, \mathbf{v} \in \mathbf{V}(h), \tag{13}$$

with a constant depending on δ_0, Ω, and the constants in Property 3.1. The bound (13) follows by proceeding as in the original proof in [3, Lemma 2.1], taking into account elliptic regularity theory for polyhedral domains and by using the anisotropic trace inequality

$$\|\varphi\|_{0,f} \leq Ch_f^{-1}\|\varphi\|_{3/2+\varepsilon,K}, \qquad \varepsilon > 0,$$

for an element $K \in \mathcal{T}$ and an entire face f of ∂K, with a constant depending on the constants in Property 3.1.

Let now $\mathbf{v} \in \mathbf{V}_h$. From (13), we obtain $|\int_\Omega \mathbf{f}\cdot\mathbf{v}\,d\mathbf{x}| \leq C\|\mathbf{f}\|_0\|\mathbf{v}\|_h$. Further, applying the discrete trace inequality from [25, Lemma 3.3] as in the proof of [25, Theorem 4.1],

$$\left|\int_{\mathcal{E}_\mathcal{B}} (\mathbf{g}\otimes\mathbf{n}) : \{\!\{\nu\nabla_h\mathbf{v}\}\!\}\,ds\right| \leq C\nu\|\delta^{\frac{1}{2}}\mathbf{g}\|_{0,\partial\Omega}\|\mathbf{v}\|_h,$$

with a constant depending on δ_0, and the constants in Property 3.1. Finally, the Cauchy-Schwarz inequality yields $|\nu \int_{\mathcal{E}_B} \delta \mathbf{g} \cdot \mathbf{v}\, ds| \leq \nu \|\delta^{\frac{1}{2}} \mathbf{g}\|_{0,\partial\Omega} \|\mathbf{v}\|_h$. This proves the assertion for F_h. Similarly, for $q \in Q_h$,

$$|G_h(q)| \leq |\int_{\mathcal{E}_B} q\, \mathbf{g} \cdot \mathbf{n}\, ds| \leq \|\delta^{\frac{1}{2}} \mathbf{g}\|_{0,\partial\Omega} \big(\int_{\mathcal{E}_B} \delta^{-1} |q|^2\, ds \big)^{\frac{1}{2}}.$$

Using again the techniques in [25, Lemma 3.3 and Theorem 4.1], we have

$$\int_{\mathcal{E}_B} \delta^{-1} |q|^2\, ds \leq C \|q\|_0^2,$$

with a constant depending on δ_0, and the constants in Property 3.1. This completes the proof. □

Remark 4.2. *The same continuity properties hold for all the functionals F_h and G_h in the mixed DG methods analyzed in [24].*

5 Generalized inf-sup condition on geometric meshes

Our main result establishes a generalized inf-sup condition on geometric meshes. To this end, we introduce the following seminorm on Q_h

$$|q|_{\mathcal{F}_\mathcal{I}}^2 := \int_{\mathcal{F}_\mathcal{I}} \gamma\, |[\![q]\!]|^2\, ds,$$

with γ the pressure stabilization function defined in (12).

We have the following result.

Theorem 5.1. *Let $\mathcal{T}$ be a geometric edge mesh $\mathcal{T}_{edge}^{n,\sigma}$ or a geometric boundary layer mesh $\mathcal{T}_{bl}^{n,\sigma}$, with a grading factor $\sigma \in (0,1)$ and n levels of refinement. Let the stabilization functions δ and γ be defined according to (10), (11), and (12). Then, there exists a constant $C > 0$ that depends on δ_0, γ_0, and the constants in Property 3.1 and (9), but is independent of ν, k, ℓ, n, and the aspect ratio of $\mathcal{T}$, such that, for any n and $k \geq 1$, $\ell = k$ or $\ell = k-1$,*

$$\sup_{0 \neq \mathbf{v} \in \mathbf{V}_h} \frac{B_h(\mathbf{v}, q)}{\|\mathbf{v}\|_h} \geq C k^{-\frac{1}{2}} \|q\|_0 \big(1 - \frac{|q|_{\mathcal{F}_\mathcal{I}}}{\|q\|_0}\big), \qquad \forall q \in Q_h \setminus \{0\}.$$

Remark 5.1. *For h-version DG approximations on shape-regular meshes, the generalized inf-sup condition in Theorem 5.1 was established in [11, 10] for LDG discretizations, in a form that also involves the auxiliary stresses present in the LDG approach. Similar inf-sup conditions also play an important role in the analysis of conforming stabilized mixed methods; see, e.g., [15, 14] and the references therein.*

The proof of Theorem 5.1 is carried out in the rest of this section. We begin by collecting several properties of L^2-projections in section 5.1 and derive bounds for averages and jumps over faces of geometric meshes in section 5.2. We then complete the proof of Theorem 5.1 in section 5.3.

5.1 L^2-projections

For an interval $I_x = (x_1, x_2)$, let $\Pi_x : L^2(I_x) \to \mathbb{Q}_k(I_x)$ denote the one-dimensional L^2-projection onto the space $\mathbb{Q}_k(I_x)$ of polynomials of degree at most k on I_x; given $v \in L^2(I_x)$, this projection is defined by imposing

$$\int_{I_x} \Pi_x v \, \varphi \, dx = \int_{I_x} v \, \varphi \, dx, \qquad \forall \varphi \in \mathbb{Q}_k(I_x).$$

The L^2-projection is stable:

$$\|\Pi_x v\|_{0,I_x} \leq \|v\|_{0,I_x}, \qquad \forall v \in L^2(I_x). \tag{14}$$

Moreover, applying similar techniques as in [8, Theorem 2.2], we have, for $k \geq 1$,

$$|\Pi_x v|_{1,I_x} \leq C k^{\frac{1}{2}} |v|_{1,I_x}, \qquad \forall v \in H^1(I_x), \tag{15}$$

with a constant $C > 0$ independent of k, I_x, and v.

We next recall the following approximation result from [19, Lemma 3.5].

Lemma 5.1. *Let $I_x = (x_1, x_2)$, $h_x = x_2 - x_1$ and $v \in H^1(I_x)$. Then, there holds*

$$|v(x_1) - \Pi_x v(x_1)|^2 + |v(x_1) - \Pi_x v(x_2)|^2 \leq C \, h_x k^{-1} \, \|v'\|^2_{0,I_x},$$

for $k \geq 1$ and with a constant $C > 0$ independent of h_x, k, and v.

We will also make use of an approximation result from [19, Lemma 3.9] for the two-dimensional L^2-projection $\Pi_x \otimes \Pi_y$; here, the subscripts indicate the variables the projectors Π_x and Π_y act on.

Lemma 5.2. *Let $I_x = (x_1, x_2)$, $I_y = (y_1, y_2)$, $h_x = x_2 - x_1$ and $h_y = y_2 - y_1$. Assume that there exists a constant $c > 0$ such that $c h_x \leq h_y \leq c^{-1} h_x$. Then, for $v \in H^1(I_x \times I_y)$ and $k \geq 1$, we have*

$$\|v - \Pi_x \otimes \Pi_y \, v\|^2_{0,\partial(I_x \times I_y)} \leq C \, h_x k^{-1} \, |v|^2_{1,I_x \times I_y},$$

with a constant $C > 0$ depending on c, but independent of h_x, h_y, k, and v.

For an axiparallel element $K_{xyz} = (x_1, x_2) \times (y_1, y_2) \times (z_1, z_2)$, the L^2-projector $\Pi_{K_{xyz}} : L^2(K_{xyz}) \to \mathbb{Q}_k(K_{xyz})$ is the product operator $\Pi_{K_{xyz}} = \Pi_x \otimes \Pi_y \otimes \Pi_z$ of one-dimensional L^2-projections. For $v \in L^2(K_{xyz})$, it satisfies

$$\int_{K_{xyz}} \Pi_{K_{xyz}} v \, \varphi \, d\mathbf{x} = \int_{K_{xyz}} v \, \varphi \, d\mathbf{x}, \qquad \forall \varphi \in \mathbb{Q}_k(K_{xyz}).$$

For an element K of a geometric edge or boundary layer mesh $\mathcal{T}$, the L^2-projection $\Pi_K : L^2(K) \to \mathbb{Q}_k(K)$ is defined by

$$\int_K \Pi_K v \, \varphi \, d\mathbf{x} = \int_K v \, \varphi \, d\mathbf{x}, \qquad \forall \varphi \in \mathbb{Q}_k(K).$$

Thanks to Property 3.1, we have $K = F_K(K_{xyz})$ for an axiparallel element $K_{xyz} = (x_1, x_2) \times (y_1, y_2) \times (z_1, z_2)$. For $v \in L^2(K)$, we therefore have

$$\Pi_K v \circ F_K \;=\; \Pi_{K_{xyz}}\big[v \circ F_K\big], \qquad \text{on } K_{xyz}. \tag{16}$$

We have the following stability result.

Lemma 5.3. *Let $\mathcal{T}$ be a geometric edge or boundary layer mesh. Let $K \in \mathcal{T}$ and $v \in H^1(K)$. Then we have for $k \geq 1$*

$$|\Pi_K v|_{1,K} \leq C k^{\frac{1}{2}} |v|_{1,K},$$

with a constant $C > 0$ depending on the bounds in Property 3.1, but independent of k, K, and v.

Proof. Let $K = K_{xyz}$ according to Property 3.1. The bounds (14) and (15) imply that

$$\begin{aligned}
\|\partial_x \Pi_{K_{xyz}} v\|_{0,K_{xyz}} &\leq C k^{\frac{1}{2}} \|\partial_x v\|_{0,K_{xyz}}, \\
\|\partial_y \Pi_{K_{xyz}} v\|_{0,K_{xyz}} &\leq C k^{\frac{1}{2}} \|\partial_y v\|_{0,K_{xyz}}, \\
\|\partial_z \Pi_{K_{xyz}} v\|_{0,K_{xyz}} &\leq C k^{\frac{1}{2}} \|\partial_z v\|_{0,K_{xyz}},
\end{aligned}$$

for any $v \in H^1(K_{xyz})$, with a constant $C > 0$ independent of k, K_{xyz}, and v. A scaling argument and the bounds in Property 3.1 prove the assertion for a general element K. □

Finally, the L^2-projection $\Pi : L^2(\Omega) \to \{v \in L^2(\Omega) : v|_K \in \mathbb{Q}_k(K),\ K \in \mathcal{T}\}$ is defined elementwise by $\Pi v|_K = \Pi_K v|_K$, $K \in \mathcal{T}$. For vector fields, we use bold-face notation (such as $\mathbf{\Pi}_{K_{xyz}}$, $\mathbf{\Pi}_K$, and $\mathbf{\Pi}$) to denote the L^2-projections that are applied componentwise.

5.2 Auxiliary results

In this section, we derive bounds for the averages and jumps over faces. We start by considering interior faces.

5.2.1 Interior faces

Let K and K' be two elements of a geometric mesh with entire faces f and f' that share an interior face $f \cap f'$ in $\mathcal{F}_\mathcal{I}$. We may assume that $f \cap f'$ is an entire face of K, that is, $f \cap f' = f$. By Property 3.1, we have $K = F_K(K_{xyz})$ and $K' = F_{K'}(K'_{xyz})$ with, e.g.,

$$K_{xyz} = (x_1, x_2) \times (y_1, y_2) \times (z_1, z_2), \qquad K'_{xyz} = (x_2, x_3) \times (y_1, y_3) \times (z_1, z_2),$$

and $y_2 \leq y_3$. The face f is then given by $f = F_f(f_{yz})$, with $f_{yz} = \{x_2\} \times (y_1, y_2) \times (z_1, z_2)$, and $F_f(y, z) = F_K(x_2, y, z) = F_{K'}(x_2, y, z)$ for $y_1 \leq y \leq y_2$,

$z_1 \le z \le z_2$. Similarly, we have $f' = F_{f'}(f'_{yz})$. For a function $\mathbf{v} \in H^1(K \cup K')^3$, we define $\mathbf{v}_{xyz} = \mathbf{v}|_K \circ F_K$ and $\mathbf{v}'_{xyz} = \mathbf{v}|_{K'} \circ F_{K'}$.

We set $h_x = x_2 - x_1$, $h'_x = x_3 - x_2$, $h_y = y_2 - y_1$, $h'_y = y_3 - y_1$, and $h_z = z_2 - z_1$, and may assume that

$$ch_x \le h'_x \le c^{-1}h_x, \tag{17}$$

according to (9). In the case where the elements K and K' match regularly (i.e., $f = f'$) the ratios of the mesh-sizes h_x, h_y and h_z can be arbitrary. However, when K and K' match irregularly (i.e., $f \neq f'$), it is essential to observe that, by definition of geometric meshes, we also have

$$ch_y \le h'_y \le c^{-1}h_y, \qquad ch_y \le h_x \le c^{-1}h_y, \tag{18}$$

with a constant $c > 0$ depending solely on the bounds in Property 3.1. The situation when K and K' match irregularly is shown in Figure 4. We point out that the above configuration covers all interior faces in geometric edge and boundary layer meshes.

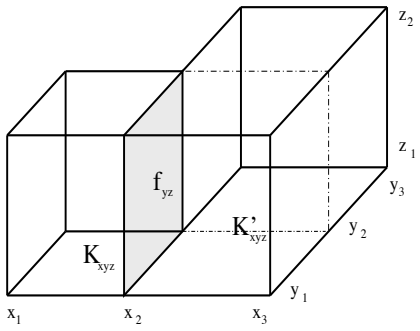

Figure 4: The axiparallel elements K_{xyz} and K'_{xyz} match irregularly. The face f_{yz} is given by $f_{yz} = \{x_2\} \times (y_1, y_2) \times (z_1, z_2)$.

We first show the following result.

Lemma 5.4. *Let $K, K' \in \mathcal{T}$ share a face $f \subset \mathcal{F}_\mathcal{I}$. Then, for $q \in Q_h$ and $\mathbf{v} \in H^1(K \cup K')^3$,*

$$\left| \int_f [\![q]\!] \cdot \{\!\{\mathbf{v} - \mathbf{\Pi v}\}\!\}\, ds \right| \le C \left(\int_f \gamma\, |[\![q]\!]|^2\, ds \right)^{\frac{1}{2}} \left(|\mathbf{v}|^2_{1,K} + |\mathbf{v}|^2_{1,K'} \right)^{\frac{1}{2}},$$

with a constant $C > 0$ that depends only on the bounds in Property 3.1 and (9).

Proof. We begin by noting that $\int_f [\![q]\!] \cdot \{\!\{\mathbf{v} - \mathbf{\Pi v}\}\!\}\, ds = \frac{1}{2}S_K + \frac{1}{2}S_{K'}$, where

$$\begin{aligned} S_K &= \int_f [\![q]\!] \cdot (\mathbf{v}|_K - \mathbf{\Pi}_K \mathbf{v}|_K)\, ds, \\ S_{K'} &= \int_f [\![q]\!] \cdot (\mathbf{v}|_{K'} - \mathbf{\Pi}_{K'} \mathbf{v}|_{K'})\, ds. \end{aligned}$$

Step 1: We start by bounding the term S_K. Setting $\mathbf{q}_{yz} = [\![q]\!] \circ F_f$, we obtain

$$\begin{aligned} S_K &= \int_f [\![q]\!] \cdot (\mathbf{v}|_K - \mathbf{\Pi}_K \mathbf{v}|_K)\, ds \\ &= \int_{f_{yz}} \mathbf{q}_{yz} \cdot (\mathbf{v}_{xyz} - \mathbf{\Pi}_{K_{xyz}} \mathbf{v}_{xyz})\, |\det(DF_f)|\, dy\, dz \\ &= \int_{f_{yz}} \mathbf{q}_{yz} \cdot (\mathbf{v}_{xyz} - \mathbf{\Pi}_x \otimes \mathbf{\Pi}_y \otimes \mathbf{\Pi}_z \mathbf{v}_{xyz})\, |\det(DF_f)|\, dy\, dz \\ &= \int_{f_{yz}} \mathbf{q}_{yz} \cdot (\mathbf{\Pi}_y \otimes \mathbf{\Pi}_z \mathbf{v}_{xyz} - \mathbf{\Pi}_x \otimes \mathbf{\Pi}_y \otimes \mathbf{\Pi}_z \mathbf{v}_{xyz})\, |\det(DF_f)|\, dy\, dz. \end{aligned}$$

Here, we have used identity (16), the factorization $\mathbf{\Pi}_{K_{xyz}} = \mathbf{\Pi}_x \otimes \mathbf{\Pi}_y \otimes \mathbf{\Pi}_z$ into one-dimensional L^2-projections, and the fact that each component of $\mathbf{q}_{yz}$ is a polynomial of degree $\ell = k$ or $\ell = k-1$ in y- and z-direction. The Cauchy-Schwarz inequality, the definition of h_f in (9), the definition of γ in (12), and (17) yield

$$S_K \le T_K \bigg(\int_{f_{yz}} h_x \max\{1,\ell\}^{-1} |\mathbf{q}_{yz}|^2\, |\det(DF_f)|\, dy\, dz \bigg)^{\frac{1}{2}} \le C \cdot T_K \cdot \bigg(\int_f \gamma |[\![q]\!]|^2\, ds \bigg)^{\frac{1}{2}},$$

with the term T_K given by

$$T_K^2 := \max\{1,\ell\} h_x^{-1} \int_{f_{yz}} |\, \mathbf{\Pi}_y \otimes \mathbf{\Pi}_z \mathbf{v}_{xyz} - \mathbf{\Pi}_x \otimes \mathbf{\Pi}_y \otimes \mathbf{\Pi}_z \mathbf{v}_{xyz}\, |^2\, |\det(DF_f)|\, dy\, dz.$$

From the stability of the one-dimensional projections $\mathbf{\Pi}_y$ and $\mathbf{\Pi}_z$ in (14) (taking into account that $|\det(DF_f)|$ is constant), the approximation result in Lemma 5.1, and the bounds in Property 3.1, we obtain

$$\begin{aligned} T_K^2 &\le \max\{1,\ell\} h_x^{-1} |\det(DF_f)| \int_{f_{yz}} |\, \mathbf{v}_{xyz} - \mathbf{\Pi}_x \mathbf{v}_{xyz}\, |^2\, dy\, dz \\ &\le C \max\{1,\ell\} k^{-1}\, |\det(DF_f)|\, \|\partial_x \mathbf{v}_{xyz}\|^2_{0,K_{xyz}} \\ &\le C\, |\det(DF_f)|\, \|DF_K\|\, |\det(DF_K^{-1})|\, |\mathbf{v}|^2_{1,K} \le C\, |\mathbf{v}|^2_{1,K}. \end{aligned}$$

Combining the above estimates shows that

$$S_K \le C\, |\mathbf{v}|_{1,K} \bigg(\int_f \gamma\, |[\![q]\!]|^2\, ds \bigg)^{\frac{1}{2}}, \tag{19}$$

with a constant C depending solely on the bounds in Property 3.1 and (9).

Step 2: Let us now consider the term $S_{K'}$. We note that there is an entire face f' of K', such that $f = f \cap f'$. If $f = f'$, then $S_{K'}$ can be bounded as S_K in Step 1. Thus, we only need to consider the case where f is an irregular face of K', i.e., f is a proper subset of f' as in Figure 4. As in the proof of Step 1,

since $\mathbf{q}_{yz}$ is a polynomial in z-direction, we have:

$$\begin{aligned} S_{K'} &= \int_f [\![q]\!] \cdot (\mathbf{v}|_{K'} - \mathbf{\Pi}_{K'}\mathbf{v}|_{K'})\, ds \\ &= \int_{f_{yz}} \mathbf{q}_{yz} \cdot (\mathbf{v}'_{xyz} - \mathbf{\Pi}_{K'_{xyz}}\mathbf{v}'_{xyz})\, |\det(DF_f)|\, dy\, dz \\ &= \int_{f_{yz}} \mathbf{q}_{yz} \cdot (\mathbf{\Pi}'_z\mathbf{v}'_{xyz}\mathbf{v}'_{xyz} - \mathbf{\Pi}'_x \otimes \mathbf{\Pi}'_y \otimes \mathbf{\Pi}'_z\mathbf{v}'_{xyz})\, |\det(DF_f)|\, dy\, dz. \end{aligned}$$

Here, we denote by $\mathbf{\Pi}'_x$, $\mathbf{\Pi}'_y$, and $\mathbf{\Pi}'_z$ the one-dimensional L^2-projections on K'_{xyz}. We obtain

$$S_{K'} \le C \cdot T_{K'} \cdot \left(\int_f \gamma\, |[\![q]\!]|^2\, ds \right)^{\frac{1}{2}},$$

with the term $T_{K'}$ given by

$$T^2_{K'} := \max\{1, \ell\} h_x^{-1} \int_{f_{yz}} |\, \mathbf{\Pi}'_z\mathbf{v}'_{xyz} - \mathbf{\Pi}'_x \otimes \mathbf{\Pi}'_y \otimes \mathbf{\Pi}'_z\mathbf{v}'_{xyz}\, |^2\, |\det(DF_f)|\, dy\, dz.$$

From the stability (14) of $\mathbf{\Pi}'_z$ in z-direction, (17), (18) and Lemma 5.2, we obtain

$$\begin{aligned} T^2_{K'} &\le \max\{1, \ell\} h_x^{-1} |\det(DF_f)| \int_{f'_{yz}} |\, \mathbf{v}'_{xyz} - \mathbf{\Pi}'_x \otimes \mathbf{\Pi}'_y\mathbf{v}'_{xyz}\, |^2\, dy\, dz \\ &\le C|\mathbf{v}'_{xyz}|^2_{1,K'_{xyz}} \le |\mathbf{v}|^2_{1,K'}. \end{aligned}$$

Combining the bounds above gives

$$S_{K'} \le C\, |\mathbf{v}|_{1,K'} \left(\int_f \gamma\, |[\![q]\!]|^2\, ds \right)^{\frac{1}{2}}, \tag{20}$$

with a constant $C > 0$ depending on the bounds in Property 3.1 and (9). Combining (19) and (20) concludes the proof. □

Next, we estimate the jump of the L^2-projection over the face f.

Lemma 5.5. *Let $K, K' \in \mathcal{T}$ share a face $f \subset \mathcal{F}_\mathcal{I}$. Suppose that $f = f \cap f'$, with f and f' entire faces of K and K', respectively. Then, for $\mathbf{v} \in H^1(K \cup K')^3$,*

$$\int_f |\underline{[\![\mathbf{\Pi}\mathbf{v}]\!]}|^2\, ds \;\le\; C \min\{h_f, h_{f'}\} k^{-1} \big[|\mathbf{v}|^2_{1,K} + |\mathbf{v}|^2_{1,K'} \big],$$

with a constant $C > 0$ that depends only on the bounds in Property 3.1 and (9).

Proof. Equality (16) ensures that

$$\begin{aligned} \int_f |\underline{[\![\mathbf{\Pi}\mathbf{v}]\!]}|^2\, ds &\le \int_f |\mathbf{\Pi}_K \mathbf{v}_{|_K} - \mathbf{\Pi}_{K'}\mathbf{v}_{|_{K'}}|^2\, ds \\ &= \int_{f_{yz}} |\mathbf{\Pi}_{K_{xyz}}\mathbf{v}_{xyz} - \mathbf{\Pi}_{K'_{xyz}}\mathbf{v}'_{xyz}|^2\, |\det(DF_f)|\, dy\, dz. \end{aligned}$$

We consider two cases separately.

Case 1: Let K and K' match regularly, i.e., $f = f'$. Since $\mathbf{v}_{xyz}$ and $\mathbf{v}'_{xyz}$ coincide on the face f_{yz}, we have $\mathbf{\Pi}_y \otimes \mathbf{\Pi}_z \mathbf{v}_{xyz} = \mathbf{\Pi}'_y \otimes \mathbf{\Pi}'_z \mathbf{v}'_{xyz}$ on f_{yz}. We thus obtain from the triangle inequality

$$\int_f |\underline{[\![\mathbf{\Pi v}]\!]}|^2 \, ds \;\leq\; C \cdot |\det(DF_f)| \;\cdot [\, T_K + T_{K'} \,],$$

with

$$\begin{aligned} T_K &= \int_{f_{yz}} |\mathbf{\Pi}_y \otimes \mathbf{\Pi}_z \mathbf{v}_{xyz} - \mathbf{\Pi}_x \otimes \mathbf{\Pi}_y \otimes \mathbf{\Pi}_z \mathbf{v}_{xyz}|^2 \, dy \, dz, \\ T_{K'} &= \int_{f_{yz}} |\mathbf{\Pi}'_y \otimes \mathbf{\Pi}'_z \mathbf{v}'_{xyz} - \mathbf{\Pi}'_x \otimes \mathbf{\Pi}'_y \otimes \mathbf{\Pi}'_z \mathbf{v}'_{xyz}|^2 \, dy \, dz. \end{aligned}$$

Using the stability (14) of the projections $\mathbf{\Pi}_y$ and $\mathbf{\Pi}_z$ in y- and z-directions, as well as the approximation result in Lemma 5.1, we obtain

$$T_K \leq C h_x k^{-1} \|\partial_x \mathbf{v}_{xyz}\|^2_{0,K_{xyz}} \leq C h_f k^{-1} |\mathbf{v}|^2_{1,K}.$$

An analogous bound for $T_{K'}$ and (17) prove the assertion in this case.

Case 2: Assume that K and K' are non-matching ($f \neq f'$). We then have that $\mathbf{\Pi}_z \mathbf{v}_{xyz} = \mathbf{\Pi}'_z \mathbf{v}'_{xyz}$ on f_{yz}. Thus,

$$\int_f |\underline{[\![\mathbf{\Pi v}]\!]}|^2 \, ds \;\leq\; C \cdot |\det(DF_f)| \;\cdot [\, T_K + T_{K'} \,],$$

with

$$\begin{aligned} T_K &= \int_{f_{yz}} |\mathbf{\Pi}_z \mathbf{v}_{xyz} - \mathbf{\Pi}_x \otimes \mathbf{\Pi}_y \otimes \mathbf{\Pi}_z \mathbf{v}_{xyz}|^2 \, dy \, dz, \\ T_{K'} &= \int_{f_{yz}} |\mathbf{\Pi}'_z \mathbf{v}'_{xyz} - \mathbf{\Pi}'_x \otimes \mathbf{\Pi}'_y \otimes \mathbf{\Pi}'_z \mathbf{v}'_{xyz}|^2 \, dy \, dz. \end{aligned}$$

Since the underlying elements are shape-regular in x- and y-directions thanks to (17) and (18), we can invoke the stability (14) of $\mathbf{\Pi}_z$ and the approximation result in Lemma 5.2. This gives

$$\begin{aligned} T_{K'} &\leq \int_{f_{yz}} |\mathbf{v}'_{xyz} - \mathbf{\Pi}'_x \otimes \mathbf{\Pi}'_y \mathbf{v}'_{xyz}|^2 \, dy \, dz \\ &\leq \int_{f'_{yz}} |\mathbf{v}'_{xyz} - \mathbf{\Pi}'_x \otimes \mathbf{\Pi}'_y \mathbf{v}'_{xyz}|^2 \, dy \, dz \\ &\leq C h'_x k^{-1} |\mathbf{v}'_{xyz}|^2_{1,K'_{xyz}} \leq C h_{f'} k^{-1} |\mathbf{v}|^2_{1,K'}. \end{aligned}$$

An analogous bound for T_K and (17) prove the assertion in this case. □

5.2.2 Boundary faces

We conclude by stating an analogous result for boundary faces that can be proved with exactly the same techniques. Let K be an element on the boundary and f an entire face of K in $\mathcal{F}_{\mathcal{B}}$.

Lemma 5.6. *For $\mathbf{v} \in H_0^1(K)^3$, we have*

$$\int_f |\underline{[\![\mathbf{\Pi v}]\!]}|^2 \, ds \leq C \, h_f k^{-1} \, |\mathbf{v}|_{1,K}^2,$$

with a constant $C > 0$ depending on the bounds in Property 3.1.

5.3 Proof of Theorem 5.1

Fix $q \in Q_h$. From the continuous inf-sup condition (2), there exists a field $\mathbf{w} \in H_0^1(\Omega)^3$ such that

$$-\int_\Omega q \nabla \cdot \mathbf{w} \, d\mathbf{x} = \|q\|_0^2, \qquad |\mathbf{w}|_1 \leq C_\Omega^{-1} \|q\|_0, \tag{21}$$

where $C_\Omega > 0$ is the continuous inf-sup constant. We then set $\mathbf{v} = \mathbf{\Pi w}$, with $\mathbf{\Pi}$ the L^2-projection defined in section 5.1. Using $[\![\mathbf{w}]\!] = 0$ on $\mathcal{F}$, (21), integration by parts, and the properties of the L^2-projection, we find

$$\begin{aligned} B_h(\mathbf{v}, q) &= B_h(\mathbf{w}, q) + B_h(\mathbf{\Pi w} - \mathbf{w}, q) \\ &= \|q\|_0^2 + \int_\Omega \nabla_h q \cdot (\mathbf{\Pi w} - \mathbf{w}) \, d\mathbf{x} - \int_{\mathcal{F}_\mathcal{I}} [\![q]\!] \cdot \{\!\{\mathbf{\Pi w} - \mathbf{w}\}\!\} \, ds \\ &= \|q\|_0^2 + \int_{\mathcal{F}_\mathcal{I}} [\![q]\!] \cdot \{\!\{\mathbf{w} - \mathbf{\Pi w}\}\!\} \, ds. \end{aligned}$$

Applying Lemma 5.4 gives

$$\begin{aligned} \left| \int_{\mathcal{F}_\mathcal{I}} [\![q]\!] \cdot \{\!\{\mathbf{w} - \mathbf{\Pi w}\}\!\} \, ds \right| &\leq \sum_{f \subset \mathcal{F}_\mathcal{I}} \left| \int_f [\![q]\!] \cdot \{\!\{\mathbf{w} - \mathbf{\Pi w}\}\!\} \, ds \right| \\ &\leq C \Big(\sum_{K \in \mathcal{T}} |\mathbf{w}|_{1,K}^2 \Big)^{\frac{1}{2}} \Big(\sum_{f \subset \mathcal{F}_\mathcal{I}} \int_f \gamma |[\![q]\!]|^2 \, ds \Big)^{\frac{1}{2}} \\ &\leq C |\mathbf{w}|_1 |q|_{\mathcal{F}_\mathcal{I}}. \end{aligned}$$

Combining the above estimates with (21) yields

$$B_h(\mathbf{v}, q) \geq C \|q\|_0^2 \left(1 - \frac{|q|_{\mathcal{F}_\mathcal{I}}}{\|q\|_0} \right), \tag{22}$$

with a constant $C > 0$ solely depending on C_Ω, and the bounds in Property 3.1 and (9).

We have from Lemma 5.3, Lemma 5.5 and Lemma 5.6, together with the definition of the discontinuity stabilization function δ,

$$\begin{aligned}\|\mathbf{v}\|_h^2 &= \sum_{K\in\mathcal{T}} |\mathbf{\Pi w}|_{1,K}^2 + \sum_{f\subset\mathcal{F}} \int_f \delta\, |\underline{[\![\mathbf{\Pi w}]\!]}|^2\, ds \\ &\leq Ck \sum_{K\in\mathcal{T}} |\mathbf{w}|_{1,K}^2 + Ck \sum_{K\in\mathcal{T}} |\mathbf{w}|_{1,K}^2 \leq Ck|\mathbf{w}|_1^2.\end{aligned}$$

Thus, invoking (21),

$$\|\mathbf{v}\|_h \leq Ck^{\frac{1}{2}} \|q\|_0. \tag{23}$$

Combining (22) and (23) concludes the proof of Theorem 5.1.

6 Global stability and a-priori error estimates

In this section, we show how the results in section 4 and section 5 can be used to obtain a global stability result and to derive a-priori error estimates. The technique we use is closely related to that used in the analysis of conforming stabilized mixed methods; see, e.g., [15, 14] and the references therein.

6.1 Global stability

Let $\mathbf{W}_h$ be the product space $\mathbf{W}_h = \mathbf{V}_h \times Q_h$, endowed with the norm

$$|\!|\!|(\mathbf{v},q)|\!|\!|_{DG}^2 = \nu\|\mathbf{v}\|_h^2 + \nu^{-1}k^{-1}\|q\|_0^2 + \nu^{-1}|q|_{\mathcal{F}_\mathcal{I}}^2.$$

In $\mathbf{W}_h$ we define the forms

$$\begin{aligned}\mathcal{A}_h(\mathbf{u},p;\mathbf{v},q) &= \widetilde{A}_h(\mathbf{u},\mathbf{v}) + \widetilde{B}_h(\mathbf{v},p) - \widetilde{B}_h(\mathbf{u},q) + C_h(p,q), \\ \mathcal{L}_h(\mathbf{v},q) &= F_h(\mathbf{v}) + G_h(q),\end{aligned}$$

and reformulate (8) equivalently as: find $(\mathbf{u}_h, p_h) \in \mathbf{W}_h$ such that

$$\mathcal{A}_h(\mathbf{u}_h,p_h;\mathbf{v},q) = \mathcal{L}_h(\mathbf{v},q) \tag{24}$$

for all $(\mathbf{v},q) \in \mathbf{W}_h$.

The following stability result holds.

Theorem 6.1. *Let $\mathcal{T}$ be a geometric edge mesh $\mathcal{T}_{edge}^{n,\sigma}$ or a geometric boundary layer mesh $\mathcal{T}_{bl}^{n,\sigma}$, with a grading factor $\sigma \in (0,1)$ and n levels of refinement. Let the stabilization functions δ and γ be defined according to (10), (11), and (12). Then, there exists a constant $C > 0$ that depends on δ_0, γ_0, and the constants in Property 3.1 and (9), but is independent of ν, k, ℓ, n, and the aspect ratio of of $\mathcal{T}$, such that, for any n and $k \geq 1$, $\ell = k$ or $\ell = k-1$,*

$$\inf_{(\mathbf{0},0)\neq(\mathbf{u},p)\in\mathbf{W}_h} \sup_{(\mathbf{0},0)\neq(\mathbf{v},q)\in\mathbf{W}_h} \frac{\mathcal{A}_h(\mathbf{u},p;\mathbf{v},q)}{|\!|\!|(\mathbf{u},p)|\!|\!|_{DG}\, |\!|\!|(\mathbf{v},q)|\!|\!|_{DG}} \geq C.$$

Proof. Fix $(\mathbf{0},0) \neq (\mathbf{u},p) \in \mathbf{V}_h \times Q_h$. Thanks to the coercivity of A_h in Theorem 4.1 and the definition of C_h, we have

$$\mathcal{A}_h(\mathbf{u},p;\mathbf{u},p) \geq \nu\beta\|\mathbf{u}\|_h^2 + \nu^{-1}|p|_{\mathcal{F}_\mathcal{I}}^2. \tag{25}$$

Furthermore, Theorem 5.1 guarantees the existence of a velocity $\mathbf{w} \in \mathbf{V}_h$ satisfying

$$B_h(\mathbf{w},p) \geq C\|p\|_0^2 - C|p|_{\mathcal{F}_\mathcal{I}}\|p\|_0, \qquad \|\mathbf{w}\|_h \leq Ck^{\frac{1}{2}}\|p\|_0. \tag{26}$$

From the definition of $\mathcal{A}_h$, the continuity properties in Theorem 4.1, weighted Cauchy-Schwarz inequalities, and (26), we obtain

$$\begin{aligned}\mathcal{A}_h(\mathbf{u},p;\mathbf{w},0) &= A_h(\mathbf{u},\mathbf{w}) + B_h(\mathbf{w},p)\\ &\geq -C\varepsilon_1\nu\|\mathbf{u}\|_h^2 - C\varepsilon_1^{-1}\nu\|\mathbf{w}\|_h^2 + C\|p\|_0^2 - C\varepsilon_2^{-1}\|p\|_0^2 - C\varepsilon_2|p|_{\mathcal{F}_\mathcal{I}}^2\\ &\geq C(1-\varepsilon_2^{-1}-\nu\varepsilon_1^{-1}k)\|p\|_0^2 - C\varepsilon_1\nu\|\mathbf{u}\|_h^2 - C\varepsilon_2|p|_{\mathcal{F}_\mathcal{I}}^2, \end{aligned}\tag{27}$$

with parameters $\varepsilon_1, \varepsilon_2 > 0$ at our disposal. We next set $(\mathbf{v},q) = (\mathbf{u},p)+\varepsilon_3(\mathbf{w},0)$, with $\varepsilon_3 > 0$. Then, combining (25) and (27), yields

$$\mathcal{A}_h(\mathbf{u},p;\mathbf{v},q) \geq C\nu(1-\varepsilon_1\varepsilon_3)\|\mathbf{u}\|_h^2 + C(\nu^{-1}-\varepsilon_3\varepsilon_2)|p|_{\mathcal{F}_\mathcal{I}}^2 + C\varepsilon_3(1-\varepsilon_2^{-1}-\nu\varepsilon_1^{-1}k)\|p\|_0^2.$$

It is now easy to see that one can select ε_1 of order $\mathcal{O}(k\nu)$, ε_2 of order $\mathcal{O}(k)$, and ε_3 of order $\mathcal{O}(\nu^{-1}k^{-1})$, respectively, in such a way that

$$\mathcal{A}_h(\mathbf{u},p;\mathbf{v},q) \geq C\nu\|\mathbf{u}\|_h^2 + C\nu^{-1}|p|_{\mathcal{F}_\mathcal{I}}^2 + C\nu^{-1}k^{-1}\|p\|_0^2 = C|\!|\!|(\mathbf{u},p)|\!|\!|_{DG}^2. \tag{28}$$

Using the fact that ε_3 is of order $\mathcal{O}(\nu^{-1}k^{-1})$ and (26) give

$$\begin{aligned}|\!|\!|(\mathbf{v},q)|\!|\!|_{DG}^2 &\leq C\nu\|\mathbf{u}\|_h^2 + C\nu\varepsilon_3^2\|\mathbf{w}\|_h^2 + \nu^{-1}k^{-1}\|p\|_0^2 + \nu^{-1}|p|_{\mathcal{F}_\mathcal{I}}^2\\ &\leq C\nu\|\mathbf{u}\|_h^2 + C\nu^{-1}k^{-1}\|p\|_0^2 + \nu^{-1}k^{-1}\|p\|_0^2 + \nu^{-1}|p|_{\mathcal{F}_\mathcal{I}}^2\\ &\leq C|\!|\!|(\mathbf{u},p)|\!|\!|_{DG}^2. \end{aligned}\tag{29}$$

Combining (28) and (29) completes the proof. □

6.2 A-priori error estimates

In order to derive a-priori error estimates, we define $(\mathbf{u},p)$ as the exact solution of the Stokes system (1) and assume that $p \in H^1(\Omega_{\text{int}})$ in a domain $\Omega_{\text{int}} \subset \Omega$ containing all the interior faces in $\mathcal{F}_\mathcal{I}$. Thus, $[\![p]\!] = 0$ on $\mathcal{F}_\mathcal{I}$. We define $Q(h) := Q_h + H^1(\Omega_{\text{int}})$ and $\mathbf{W}(h) := \mathbf{V}(h) \times Q(h)$, equipped with the norm $|\!|\!|(\mathbf{v},q)|\!|\!|_{DG}$.

From the continuity properties in Theorem 4.1, Theorem 4.2 and the Cauchy-Schwarz inequality, it can be seen that

$$|\mathcal{A}_h(\mathbf{u},p;\mathbf{v},q)| \leq Ck^{\frac{1}{2}}\,|\!|\!|(\mathbf{u},p)|\!|\!|_{DG}\,|\!|\!|(\mathbf{v},q)|\!|\!|_{DG}, \qquad \forall(\mathbf{u},p),\ (\mathbf{v},q) \in \mathbf{W}(h), \tag{30}$$

and

$$|\mathcal{L}_h(\mathbf{v},q)| \leq C\left[\nu^{-1}\|f\|_0^2 + \nu k\|\delta^{\frac{1}{2}}\mathbf{g}\|_{0,\partial\Omega}^2\right]^{\frac{1}{2}}|\!|\!|(\mathbf{v},q)|\!|\!|_{DG}, \qquad \forall(\mathbf{v},q) \in \mathbf{W}_h, \tag{31}$$

with constants as in Theorem 4.1 and Theorem 4.2, respectively.

Taking into account (30), the global inf-sup condition in Theorem 6.1, and the non-consistency of the forms $\widetilde{A}_h$ and $\widetilde{B}_h$, we obtain straightforwardly the following a-priori bound.

Theorem 6.1. *Let $(\mathbf{u}, p)$ be the exact solution of the Stokes system (1), with $p \in H^1(\Omega_{\text{int}})$, and let $(\mathbf{u}_h, p_h)$ be its discontinuous Galerkin approximation (6) on a geometric edge mesh $\mathcal{T} = \mathcal{T}_{edge}^{n,\sigma}$ or a geometric boundary layer mesh $\mathcal{T} = \mathcal{T}_{bl}^{n,\sigma}$, with a grading factor $\sigma \in (0,1)$ and n levels of refinement. Let the stabilization functions δ and γ be defined as in (10), (11) and (12), respectively. Then,*

$$|\!|\!|(\mathbf{u}-\mathbf{u}_h, p-p_h)|\!|\!|_{DG} \;\le\; Ck^{\frac{1}{2}} \inf_{(\mathbf{v},q)\in\mathbf{W}_h} |\!|\!|(\mathbf{u}-\mathbf{v}, p-q)|\!|\!|_{DG} + C\,\mathcal{R}_h(\mathbf{u},p),$$

with a constant $C > 0$ that depends on δ_0, γ_0, and the constants in Property 3.1 and (9), but is independent of ν, k, ℓ, n, and the aspect ratio of the anisotropic elements in $\mathcal{T}$. Here, $\mathcal{R}_h(\mathbf{u},p)$ is the residual

$$\mathcal{R}_h(\mathbf{u},p) = \sup_{(\mathbf{w},s)\in\mathbf{W}_h} \frac{|\mathcal{A}_h(\mathbf{u},p;\mathbf{w},s) - \mathcal{L}_h(\mathbf{w},s)|}{|\!|\!|(\mathbf{w},s)|\!|\!|_{DG}}.$$

Let us make precise the abstract error bound above for a smooth solution $(\mathbf{u},p) \in H^{s+1}(\Omega)^3 \times H^s(\Omega)$, $s \ge 1$, on isotropically refined meshes with mesh-size h with possible hanging nodes and for mixed-order elements where $\ell = k-1$.

In this case, the residual $\mathcal{R}_h(\mathbf{u},p)$ can be bounded (see [24, Proposition 8.1]) by

$$\mathcal{R}_h(\mathbf{u},p) \le \sup_{(\mathbf{w},s)\in\mathbf{W}_h} \frac{|\int_{\mathcal{F}} \{\!\{\nu\nabla\mathbf{u} - \underline{T}(\nu\nabla\mathbf{u})\}\!\} : \underline{[\![\mathbf{w}]\!]}\, ds| + |\int_{\mathcal{F}} \{\!\{p - T(p)\}\!\} [\![\mathbf{w}]\!]\, ds|}{|\!|\!|(\mathbf{w},s)|\!|\!|_{DG}},$$

where $\underline{T}$ and T are the L^2-projections onto $\underline{\Sigma}_h$ and Q_h, respectively. The Cauchy-Schwarz inequality and standard *hp*-approximation properties then give

$$\mathcal{R}_h(\mathbf{u},p) \le C\frac{h^{\min\{s,k\}}}{k^{s+\frac{1}{2}}}\left[\nu^{\frac{1}{2}}\|\mathbf{u}\|_{s+1} + \nu^{-\frac{1}{2}}\|q\|_s\right].$$

Furthermore,

$$\inf_{(\mathbf{v},q)\in\mathbf{W}_h} |\!|\!|(\mathbf{u}-\mathbf{v}, p-q)|\!|\!|_{DG} \le C\frac{h^{\min\{s,k\}}}{k^{s-\frac{1}{2}}}\left[\nu^{\frac{1}{2}}\|\mathbf{u}\|_{s+1} + \nu^{-\frac{1}{2}}\|q\|_s\right]$$

and thus

$$|\!|\!|(\mathbf{u}-\mathbf{u}_h, p-p_h)|\!|\!|_{DG} \le C\frac{h^{\min\{s,k\}}}{k^{s-1}}\left[\nu^{\frac{1}{2}}\|\mathbf{u}\|_{s+1} + \nu^{-\frac{1}{2}}\|q\|_s\right]. \tag{32}$$

This estimate is optimal in the mesh-size h and suboptimal in k by one power of k in the velocity and by a power $k^{3/2}$ in the pressure, respectively.

Similarly to [24, Sect. 8], we obtain a slightly better result on conforming meshes, that is,

$$|\!|\!|(\mathbf{u}-\mathbf{u}_h, p-p_h)|\!|\!|_{DG} \le C\frac{h^{\min\{s,k\}}}{k^{s-\frac{1}{2}}}\left[\nu^{\frac{1}{2}}\|\mathbf{u}\|_{s+1} + \nu^{-\frac{1}{2}}\|q\|_s\right]. \tag{33}$$

We point out that the a-priori error bounds (32) and (33) hold verbatim for equal-order elements.

Remark 6.1. *We note that the dependence on the polynomial degree k in (32) and (33) is slightly better than the hp-estimates in [24] for mixed-order* $\mathbb{Q}_k - \mathbb{Q}_{k-1}$ *elements without pressure stabilization.*

References

[1] M. Ainsworth and P. Coggins, *The stability of mixed hp–finite element methods for Stokes flow on high aspect ratio elements*, SIAM J. Numer. Anal. **38** (2000), 1721–1761.

[2] B. Andersson, U. Falk, I. Babuška, and T. von Petersdorff, *Reliable stress and fracture mechanics analysis of complex aircraft components using a hp–version FEM*, Internat. J. Numer. Methods Engrg. **38** (1995), 2135–2163.

[3] D.N. Arnold, *An interior penalty finite element method with discontinuous elements*, SIAM J. Numer. Anal. **19** (1982), 742–760.

[4] D.N. Arnold, F. Brezzi, B. Cockburn, and L.D. Marini, *Unified analysis of discontinuous Galerkin methods for elliptic problems*, SIAM J. Numer. Anal. **39** (2001), 1749–1779.

[5] I. Babuška and B. Guo, *Approximation properties of the hp–version of the finite element method*, Comput. Methods Appl. Mech. Engrg. **133** (1996), 319–346.

[6] G.A. Baker, W.N. Jureidini, and O.A. Karakashian, *Piecewise solenoidal vector fields and the Stokes problem*, SIAM J. Numer. Anal. **27** (1990), 1466–1485.

[7] F. Brezzi and M. Fortin, *Mixed and hybrid finite element methods*, Springer Series in Computational Mathematics, vol. 15, Springer–Verlag, New York, 1991.

[8] C. Canuto and A. Quarteroni, *Approximation results for orthogonal polynomials in Sobolev spaces*, Math. Comp. **38** (1982), 67–86.

[9] B. Cockburn, *Discontinuous Galerkin methods for convection-dominated problems*, High-Order Methods for Computational Physics (T. Barth and H. Deconink, eds.), vol. 9, Springer–Verlag, New York, 1999, pp. 69–224.

[10] B. Cockburn, G. Kanschat, and D. Schötzau, *The local discontinuous Galerkin method for the Oseen equations*, Tech. Report 02-05, Department of Mathematics, University of Basel, 2002.

[11] B. Cockburn, G. Kanschat, D. Schötzau, and C. Schwab, *Local discontinuous Galerkin methods for the Stokes system*, SIAM J. Numer. Anal. **40** (2002), 319–343.

[12] B. Cockburn, G.E. Karniadakis, and C.-W. Shu (eds.), *Discontinuous Galerkin methods. Theory, computation and applications*, Lect. Notes Comput. Sci. Eng., vol. 11, Springer–Verlag, New York, 2000.

[13] B. Cockburn and C.-W. Shu, *Runge–Kutta discontinuous Galerkin methods for convection–dominated problems*, J. Sci. Comput. **16** (2001), 173–261.

[14] L. Franca, T. Hughes, and R. Stenberg, *Stabilized finite element methods*, Incompressible Computational Fluid Dynamics: Trends and Advances (M. Gunzburger and R. Nicolaides, eds.), Cambridge University Press, 1993, pp. 87–107.

[15] L. Franca and R. Stenberg, *Error analysis of some Galerkin-least-squares methods for the elasticity equations*, SIAM J. Numer. Anal. **28** (1991), 1680–1697.

[16] V. Girault and P.A. Raviart, *Finite element methods for Navier–Stokes equations*, Springer–Verlag, New York, 1986.

[17] V. Girault, B. Rivière, and M.F. Wheeler, *A discontinuous Galerkin method with non-overlapping domain decomposition for the Stokes and Navier-Stokes problems*, Tech. Report 02-08, TICAM, UT Austin, 2002.

[18] P. Hansbo and M.G. Larson, *Discontinuous finite element methods for incompressible and nearly incompressible elasticity by use of Nitsche's method*, Comput. Methods Appl. Mech. Engrg. **191** (2002), 1895–1908.

[19] P. Houston, C. Schwab, and E. Süli, *Discontinuous hp-finite element methods for advection–diffusion–reaction problems*, SIAM J. Numer. Anal. **39** (2002), 2133–2163.

[20] O.A. Karakashian and W.N. Jureidini, *A nonconforming finite element method for the stationary Navier-Stokes equations*, SIAM J. Numer. Anal. **35** (1998), 93–120.

[21] J.M. Melenk and C. Schwab, *hp–FEM for reaction–diffusion equations, I. Robust exponential convergence*, SIAM J. Numer. Anal. **35** (1998), 1520–1557.

[22] D. Schötzau and C. Schwab, *Mixed hp-FEM on anisotropic meshes*, Math. Models Methods Appl. Sci. **8** (1998), 787–820.

[23] D. Schötzau, C. Schwab, and R. Stenberg, *Mixed hp-FEM on anisotropic meshes, II. Hanging nodes and tensor products of boundary layer meshes*, Numer. Math. **83** (1999), 667–697.

[24] D. Schötzau, C. Schwab, and A. Toselli, *Mixed hp-DGFEM for incompressible flows*, Tech. Report 02-10, Seminar for Applied Mathematics, ETH Zürich, 2002, in press in SIAM J. on Numer. Anal.

[25] D. Schötzau, Ch. Schwab, and A. Toselli, *Mixed hp-DGFEM for incompressible flows, II: Geometric edge meshes*, Tech. Report 02-13, Department of Mathematics, University of Basel, 2002, submitted to IMA J. on Numer. Anal.

[26] C. Schwab, *p- and hp-FEM – Theory and application to solid and fluid mechanics*, Oxford University Press, Oxford, 1998.

[27] C. Schwab and M. Suri, *The p and hp version of the finite element method for problems with boundary layers*, Math. Comp. **65** (1996), 1403–1429.

[28] C. Schwab, M. Suri, and C.A. Xenophontos, *The hp–FEM for problems in mechanics with boundary layers*, Comput. Methods Appl. Mech. Engrg. **157** (1998), 311–333.

[29] A. Toselli, *HP-Discontinuous Galerkin approximations for the Stokes problem*, Math. Models Method. Appl. Sci. **12** (2002), no. 11, 1565–1616.

[30] A. Toselli and C. Schwab, *Mixed hp-finite element approximations on geometric edge and boundary layer meshes in three dimensions*, Tech. Report 01-02, Seminar for Applied Mathematics, ETH Zürich, 2001, in press in Numer. Math.

Research Reports

No.	Authors	Title
02-25	D. Schötzau, C. Schwab, A. Toselli	Mixed *hp*-DGFEM for incompressible flows III: Pressure stabilization
02-24	F.M. Buchmann, W.P. Petersen	A stochastically generated preconditioner for stable matrices
02-23	A.W. Rüegg, A. Schneebeli, R. Lauper	Generalized *hp*-FEM for Lattice Structures
02-22	L. Filippini, A. Toselli	*hp* Finite Element Approximations on Non-Matching Grids for the Stokes Problem
02-21	D. Schötzau, C. Schwab, A. Toselli	Mixed *hp*-DGFEM for incompressible flows II: Geometric edge meshes
02-20	A. Toselli, X. Vasseur	A numerical study on Neumann-Neumann and FETI methods for *hp*-approximations on geometrically refined boundary layer meshes in two dimensions
02-19	D. Schötzau, Th.P. Wihler	Exponential convergence of mixed *hp*-DGFEM for Stokes flow in polygons
02-18	P.-A. Nitsche	Sparse approximation of singularity functions
02-17	S.H. Christiansen	Uniformly stable preconditioned mixed boundary element method for low-frequency electromagnetic scattering
02-16	S.H. Christiansen	Mixed boundary element method for eddy current problems
02-15	A. Toselli, X. Vasseur	Neumann-Neumann and FETI preconditioners for *hp*-approximations on geometrically refined boundary layer meshes in two dimensions
02-14	Th.P. Wihler	Locking-Free DGFEM for Elasticity Problems in Polygons
02-13	S. Beuchler, R. Schneider, C. Schwab	Multiresolution weighted norm equivalences and applications
02-12	M. Kruzik, A. Prohl	Macroscopic modeling of magnetic hysteresis
02-11	A.-M. Matache, C. Schwab, T. von Petersdorff	Fast deterministic pricing of options on Lévy driven assets
02-10	D. Schötzau, C. Schwab, A. Toselli	Mixed *hp*-DGFEM for incompressible flows
02-09	Ph. Frauenfelder, Ch. Lage	Concepts - An object-oriented software package for partial differential equations
02-08	A.-M. Matache, J.M. Melenk	Two-Scale Regularity for Homogenization Problems with Non-Smooth Fine Scale Geometry